
JOINT MODEL FOR LONGITUDINAL AND SPATIO-TEMPORAL SURVIVAL DATA

A PREPRINT

• **Victor Medina-Olivares**

Research Center Trustworthy Data Science and Security, UA Ruhr
Department of Statistics, TU Dortmund, Dortmund, Germany
victor.medina@tu-dortmund.de

• **Finn Lindgren**

School of Mathematics, University of Edinburgh, Edinburgh, UK

• **Raffaella Calabrese**

Business School, University of Edinburgh, Edinburgh, UK

• **Jonathan Crook**

Business School, University of Edinburgh, Edinburgh, UK

Abstract

In credit risk analysis, survival models with fixed and time-varying covariates are widely used to predict a borrower's time-to-event. When the time-varying drivers are endogenous, modelling jointly the evolution of the survival time and the endogenous covariates is the most appropriate approach, also known as the joint model for longitudinal and survival data. In addition to the temporal component, credit risk models can be enhanced when including borrowers' geographical information by considering spatial clustering and its variation over time. We propose the Spatio-Temporal Joint Model (STJM) to capture spatial and temporal effects and their interaction. This Bayesian hierarchical joint model reckons the survival effect of unobserved heterogeneity among borrowers located in the same region at a particular time. To estimate the STJM model for large datasets, we consider the Integrated Nested Laplace Approximation (INLA) methodology. We apply the STJM to predict the time to full prepayment on a large dataset of 57,258 US mortgage borrowers with more than 2.5 million observations. Empirical results indicate that including spatial effects consistently improves the performance of the joint model. However, the gains are less definitive when we additionally include spatio-temporal interactions.

Keywords Discrete time-to-event · Spatio-temporal frailties · Bayesian joint model · Credit risk management

1 Introduction

Lenders build mathematical models to predict credit events like defaults and full prepayments. Survival approaches are popular in this regard, as they facilitate the inclusion of fixed and time-varying covariates (TVCs), handle censored data, and allow prediction for different time horizons (see Thomas et al., 2017). Recently, a new methodology has been introduced in this context, known as joint modelling of longitudinal and survival data (joint models hereafter, Tsiatis and Davidian, 2004; Rizopoulos, 2012). Initially developed in medical research, this methodology offers two attractive features compared to the standard survival credit risk approaches. First, when TVCs are endogenous, as typically in the case of performing covariates, joint models provide a robust statistical procedure to handle the mutual evolution of the survival process and

endogenous TVCs. Second, by jointly modelling survival and endogenous TVCs, we encounter a natural prediction framework that does not rely on lagged values or exogeneity assumptions about TVCs, as is commonly done otherwise (Crook and Bellotti, 2010). In addition, recent studies show that joint models show better prediction performance than the survival counterparts (Hu and Zhou, 2019; Medina-Olivares et al., 2023a,b).

A joint model typically comprises two sub-models: one for the survival process and another for the endogenous TVC, also referred to as the longitudinal outcome. These sub-models are connected through a latent structure, often characterised by the inclusion of random effects. In this work, we considered adaptable predictor representations within the survival process, aiming to incorporate geographical information related to borrowers. This allows us to account for spatial clustering and its variation over time, factors that hold the potential to enhance the predictive capabilities of credit risk models, as shown previously (Goodstein et al., 2017; Gupta, 2019; Calabrese and Crook, 2020; Calabrese, 2023).

We make four contributions to the literature:

1. We propose a Bayesian hierarchical joint model in discrete time, featuring a flexible baseline hazard that accommodates spatial and spatio-temporal interactions. This approach captures the survival impact of unobserved spatial variables among borrowers and enables us to leverage information from neighbouring areas. We term this model the Spatio-Temporal Joint Model (STJM).
2. To handle large datasets such as those seen in credit risk analysis, we adopt the INLA methodology (Rue et al., 2009) to estimate the STJM. This allows us to estimate the model on a dataset with more than 2.5 million observations. To our knowledge, this dataset is the largest used in the joint model literature when writing this work.
3. To compare different model specifications, we introduce a novel approximation method of the *cross-validated Dynamic Conditional Likelihood* (cvDCL, see Rizopoulos et al., 2016)¹, leveraging pre-computed quantities from the INLA methodology for efficient estimation.
4. We apply the STJM to predict full prepayment events in US mortgage loans and demonstrate that including spatial components consistently improves the performance of the joint model across all evaluation time points. Nevertheless, our empirical analysis reveals that the performance improvements are less significant when we incorporate spatio-temporal interactions in addition to the main effects.

Previous studies show that spatial contagion plays a significant role in credit risk analysis on mortgage loans. Goodstein et al. (2017) obtain that surrounding areas have a relevant impact on strategic mortgage defaults in addition to borrowers' characteristics. Strategic defaults occur when borrowers choose to default because the economic benefits outweigh the costs, unlike borrowers who default because they have an unexpected net income shock. Moreover, Guiso et al. (2013); Towe and Lawley (2013) find strong evidence that social interactions among neighbours influence the propensity for strategic defaults. There are different reasons for spatial contagion on mortgage defaults. One primary factor is the reduction of property values in a neighbourhood, which in turn is highly spatially correlated (Gelfand et al., 1998; Iversen Jr, 2001). Neighbourhood characteristics, such as increasing crime rates, vandalism, or legislative changes, can negatively impact a property value (Pence, 2006). Additionally, an increased number of defaults in certain areas can lead banks to limit credit options in these neighbours, such as renegotiations. Spatial contagion can also manifest in credit events beyond defaults. For example, Gupta (2019) discover a significant spatial dependence in early repayment activity for mortgage loans due to similar reasons highlighted before for mortgage defaults. Decreased property values in a given area could affect borrowers' inclination to seek new refinancing options. At the same time, banks might reduce credit extensions or renegotiation if they anticipate a drop in property prices or other foreclosure externalities.

Regarding survival models for predicting mortgage defaults, Calabrese and Crook (2020) is the first work to include spatial contagion. They incorporate time and spatial-varying coefficients in a survival model that predicts time to default in UK mortgage loans, showing better accuracy than relevant benchmarks. However, they do not account for possible endogeneity in the TVCs included in the model and lack a predictive framework for their future trajectories, as offered by the joint model approach.

Concerning the literature on joint models with spatial dependence, Zhou et al. (2008) introduce a joint model in continuous time to handle two related time-to-event outcomes. They assume a Weibull baseline distribution with spatially correlated frailties. Additionally, Ratcliffe et al. (2004) incorporate spatial clustering as univariate independent random effects. Building on the same principles, Martins et al. (2016) propose a joint

¹The cvDCL is a cross-entropy estimate of the cross-validators posterior predictive conditional density.

model with spatial random effects to analyse AIDS data in Brazil. In that work, they adopt an intrinsic conditional autoregressive model (ICAR, see Besag et al. (1991)) as a prior distribution for the unobserved spatial effects, which aligns with our approach. However, these papers do not explore a unified joint model encompassing discrete survival data, spatio-temporal interactions, and do not demonstrate scalability with large datasets.

The manuscript is structured as follows. In Section 2, we introduce the STJM, its estimation procedure, and the Bayesian model selection. In Section 3, we present and compare the empirical results of different joint models to predict the time to full prepayment event on US mortgages. Section 4 concludes.

2 Methodology

2.1 Spatio-Temporal Joint Model (STJM)

Consider a total of N mortgage loans with their associated properties distributed over A areas. Each area, indexed by $a = 1, \dots, A$, has a total of N_a properties, i.e. $\sum_{a=1}^A N_a = N$. For each mortgage loan i ($i = 1, \dots, N$), we are provided with the following information: the location $a_i \in \{1, \dots, A\}$; the loan origination date t^0_i ; an event indicator δ_i , which takes the value 1 if a full prepayment occurs and 0 otherwise; and the time elapsed from the loan origination to its last recorded observation time $t_i \leq T$. Here, T represents the duration of the study. We assume that at time t_i , either a full prepayment has occurred ($\delta_i = 1$), or the observation is right-censored ($\delta_i = 0$), i.e. we observe loan i until time t_i but not beyond that (Allison, 1982).

Additionally, we are provided with a vector of time-fixed covariates \mathbf{z}_i and a loan-specific covariate collected regularly at multiple points in time (in our case, every month). We represent this time-varying covariate as $y_{i,s}$, where $s = 1, \dots, t_i$. The $y_{i,s}$ values correspond to the longitudinal outcome within the framework of our joint model. We use lowercase to distinguish the realisations of random variables.

We aim to understand the relationship of these data in jointly modelling the time to event T_i and the longitudinal outcome $Y_{i,s}$ up to a given endpoint for the i -th loan associated with area a_i . The following describes the proposed approach for the longitudinal and survival processes.

Longitudinal process

Assume the longitudinal outcome $Y_{i,s}$ follows a mixed-effect model (Laird and Ware, 1982), where the predictor $\eta_{Y_{i,s}}$ is composed of fixed effects $\mathbf{q}_{i,s}^\top \boldsymbol{\beta}_1$ and random effects $\mathbf{d}_{i,s}^\top \mathbf{U}_i$. Here, $\boldsymbol{\beta}_1$ is a vector of coefficients associated with the covariates $\mathbf{q}_{i,s}$, and $\mathbf{d}_{i,s}$ is the design vector corresponding to the random effects \mathbf{U}_i of dimension r . Specifically,

$$\begin{aligned} Y_{i,s} | \eta_{Y_{i,s}}, \tau_Y &\sim N(\eta_{Y_{i,s}}, \tau_Y^{-1}) \\ \eta_{Y_{i,s}} &= \mathbf{q}_{i,s}^\top \boldsymbol{\beta}_1 + \mathbf{d}_{i,s}^\top \mathbf{U}_i \\ \mathbf{U}_i | Q_U &\sim N_r(\mathbf{0}, Q_U^{-1}), \end{aligned} \quad (1)$$

where τ_Y is the precision parameter of the error terms. We assume that \mathbf{U}_i are mutually independent among mortgage loans and distributed as a zero-mean multivariate Gaussian distribution with $r \times r$ precision matrix Q_U . Given the random effects, we consider that observations within each loan are conditionally independent. Therefore, the random effects account for the correlation between these different observations.

2.1.1 Survival process

Following the discrete-time survival formulation presented in Allison (1982), we represent the random variable T_i using a sequence of binary random variables $X_{i,s}$. These variables take the value 1 if the loan i is fully prepaid at time $s = t_i$ after origination and 0 otherwise. In the case of censored loans, the sequence will consist entirely of zeros. Conversely, for fully prepaid loans, the sequence will be composed of zeros, except for the last observation, which will take the value 1. To relate $X_{i,s}$ with the predictor $\eta_{X_{i,s}}$, we use a logit link function, which can be expressed as follows

$$\begin{aligned} X_{i,s} | \eta_{X_{i,s}} &\sim \text{Bernoulli}(\text{logit}^{-1}(\eta_{X_{i,s}})) \\ \eta_{X_{i,s}} &= \nu_{a_i,s} + \mathbf{z}_i^\top \boldsymbol{\beta}_2 + \lambda(\mathbf{d}_{i,s}^\top \mathbf{U}_i), \end{aligned} \quad (2)$$

where $\nu_{a_i,s}$ represents the baseline risk, which varies across both time and space, covering the entire discrete domain of $a_i \in \{1, \dots, A\}$ and $s \in \{1, \dots, T\}$. The vector $\boldsymbol{\beta}_2$ contains coefficients associated with the

where \mathbf{u}_{-a} represents the set of spatial effects excluding the area a . Therefore, u_a has a local mean of $\sum_{a':a\sim a'} u_{a'}/m_a$, which corresponds to the average value of spatial effects from the neighbouring areas, and its variance is inversely related to the number of neighbours, m_a . Consequently, the presence of more neighbours results in greater certainty regarding the effect.

Spatio-temporal interactions ($\delta_{a,s}$) To model the spatio-temporal interactions $\boldsymbol{\delta} = (\delta_{11}, \dots, \delta_{A1}, \dots, \delta_{1T}, \dots, \delta_{AT})^\top$, we adopt the approach presented in Clayton (1996) and further elaborated in Knorr-Held (2000). In this approach, the structure matrix R_δ can be obtained as the Kronecker product of the structure matrices from the temporal and spatial main effects, i.e. $R_\delta = R_v \otimes R_u$. As a result, the corresponding joint density is given by Schrödle and Held (2011)

$$\boldsymbol{\delta}|\tau_\delta \propto \exp\left(-\frac{\tau_\delta}{2} \sum_{s=3}^T \sum_{a\sim a'} [(\delta_{a,s} - 2\delta_{a,s-1} + \delta_{a,s-2}) - (\delta_{a',s-2} - 2\delta_{a',s-1} + \delta_{a',s})]^2\right), \quad (5)$$

where τ_δ is the corresponding precision parameter.

In the spatial literature, it is widely recognised that structured additive predictors formed by Equations 3, 4, and 5 can lead to identifiability issues (see, e.g. Knorr-Held, 2000; Goicoa et al., 2018). To ensure appropriate identifiability, we need to impose constraints on the random effects \mathbf{v} , \mathbf{u} and $\boldsymbol{\delta}$. In this regard, we follow the approach of Goicoa et al. (2018), who employ reparametrisations using spectral decomposition on the structure matrices R_v , R_u and R_δ . These reparametrisations conduct to the following constraints: $\sum_{s=1}^T v_s = 0$, $\sum_{a=1}^A u_a = 0$, $\sum_{s=1}^T \delta_{a,s} = 0$ for $a = 1, \dots, A$ and $\sum_{a=1}^A \delta_{a,s} = 0$ for $s = 1, \dots, T$.

2.2 Estimation

From Equations 1 and 2, we know that the random effects \mathbf{U}_i are shared between both the longitudinal and survival processes. The joint model approach assumes that these two processes are conditionally independent given the random effects (Wulfsohn and Tsiatis, 1997; Henderson et al., 2000; Tsiatis and Davidian, 2004). Therefore, the joint distribution of the observed values $\mathbf{y}_i = (y_{i1}, \dots, y_{i,t_i})^\top$ and $\mathbf{x}_i = (x_{i1}, \dots, x_{i,t_i})^\top$ for loan i conditional on the random effects is

$$p(\mathbf{y}_i, \mathbf{x}_i|\mathbf{U}_i, \Theta) = \prod_{s=1}^{t_i} p(y_{i,s}|\mathbf{U}_i, \Theta)p(x_{i,s}|\mathbf{U}_i, \Theta), \quad (6)$$

where Θ denotes the vector of parameters included in both processes. It follows from Equation 1 that

$$\begin{aligned} p(y_{i,s}|\mathbf{U}_i, \Theta) &= \left(\frac{\tau_Y}{2\pi}\right)^{1/2} \exp\left(-\frac{\tau_Y(y_{i,s} - \eta_{Yi,s})^2}{2}\right) \\ &= \left(\frac{\tau_Y}{2\pi}\right)^{1/2} \exp\left(-\frac{\tau_Y(y_{i,s} - \mathbf{q}_{i,s}^\top \boldsymbol{\beta}_1 - \mathbf{d}_{i,s}^\top \mathbf{U}_i)^2}{2}\right), \end{aligned}$$

and from Equation 2

$$\begin{aligned} p(x_{i,s}|\mathbf{U}_i, \Theta) &= [\text{logit}^{-1}(\eta_{Xi,s})]^{x_{i,s}} [1 - \text{logit}^{-1}(\eta_{Xi,s})]^{1-x_{i,s}} \\ &= [\text{logit}^{-1}(\nu_{a_i,s} + \mathbf{z}_i^\top \boldsymbol{\beta}_2 + \lambda(\mathbf{d}_{i,s}^\top \mathbf{U}_i))]^{x_{i,s}} \\ &\quad \times [1 - \text{logit}^{-1}(\nu_{a_i,s} + \mathbf{z}_i^\top \boldsymbol{\beta}_2 + \lambda(\mathbf{d}_{i,s}^\top \mathbf{U}_i))]^{1-x_{i,s}}. \end{aligned}$$

Hence, the contribution of the i -th loan to the observation density is

$$\begin{aligned} p(\mathbf{y}_i, \mathbf{x}_i|\Theta) &= \int p(\mathbf{y}_i, \mathbf{x}_i|\mathbf{U}_i, \Theta)p(\mathbf{U}_i|\Theta)d\mathbf{U}_i \\ &= \int \prod_{s=1}^{t_i} p(y_{i,s}|\mathbf{U}_i, \Theta)p(x_{i,s}|\mathbf{U}_i, \Theta)p(\mathbf{U}_i|\Theta)d\mathbf{U}_i, \end{aligned} \quad (7)$$

where $p(\mathbf{U}_i|\Theta)$ is as zero-mean multivariate Gaussian with precision matrix Q_U (Section 2.1), i.e. $p(\mathbf{U}_i|\Theta) = (2\pi)^{-r/2}|Q_U|^{1/2} \exp(-\mathbf{U}_i^\top Q_U \mathbf{U}_i/2)$.

Denote the complete set of observation variables as $\mathcal{D} = \{\mathbf{y}_i, \mathbf{x}_i : i = 1, \dots, N\}$. The joint posterior distribution follows $p(\Theta|\mathcal{D}) \propto p(\mathcal{D}|\Theta)p(\Theta)$, where $p(\mathcal{D}|\Theta) = \prod_i^N p(\mathbf{y}_i, \mathbf{x}_i|\Theta)$ is the overall observation density and $p(\Theta)$ the joint prior.

Theoretically, we could estimate this model specification using simulation-based schemes, as demonstrated in Medina-Olivares et al. (2023a) for the joint model with autoregressive terms. However, it should be noted that this strategy can be computationally expensive and may even become infeasible for applications dealing with large datasets. To address these computational challenges and in line with the estimation approach followed in Medina-Olivares et al. (2023b), we propose employing the INLA methodology (Rue et al., 2009).

INLA offers accurate estimations of the posterior at a considerably lower computational cost and is readily accessible through the R-INLA software package for R (<https://www.r-inla.org/>). This methodology is particularly suitable for models belonging to the class of latent Gaussian models (LGM), which is a flexible and widely used class of models. For instance, many structured Bayesian additive models fall under this category (see Fahrmeir and Tutz, 1994; Gelman et al., 2013). Importantly, the STJM also belongs to this class of models, as shown next.

We define the latent field $\boldsymbol{\mu} = (\boldsymbol{\eta}_Y, \boldsymbol{\eta}_X, \mathbf{U}, \boldsymbol{\beta}_1, \boldsymbol{\beta}_2, \nu_0, \mathbf{v}, \mathbf{u}, \boldsymbol{\delta})$, which comprises the set of unobserved variables in the STJM. The terms $\boldsymbol{\eta}_Y$ and $\boldsymbol{\eta}_X$ correspond to the predictors described in Equations 1 and 2, respectively, each having $\sum_i^N t_i$ elements. As the remaining elements are latent variables, we refer to $\boldsymbol{\mu}$ as a latent field. Additionally, since we assume that $\boldsymbol{\mu}$ follows a zero-mean multivariate Gaussian distribution, it is called a latent Gaussian field (Rue and Held, 2005).

Expressly, we assume that the coefficients $\boldsymbol{\beta}_1$, $\boldsymbol{\beta}_2$, and ν_0 follow a zero-mean Gaussian distribution with a precision matrix $\tau_f \mathbf{I}$, where \mathbf{I} is the identity matrix of the corresponding dimension, and τ_f is a precision parameter. Typically, τ_f is set as a fixed value close to zero in the model, resulting in a large prior variance.

As described in Section 2.1, the random effects $\mathbf{U}_i | Q_{\mathbf{U}} \sim N(\mathbf{0}, Q_{\mathbf{U}}^{-1})$, and the terms \mathbf{v} , \mathbf{u} , and $\boldsymbol{\delta}$ have priors with Gaussian kernels (see Equations 3, 4, and 5, respectively). Consequently, the precision matrix of the latent Gaussian field $\boldsymbol{\mu}$, which includes all the individual precision matrices, is denoted as $Q(\boldsymbol{\theta}_1)$, where $\boldsymbol{\theta}_1$ is the corresponding set of hyperparameters. In our case, $\boldsymbol{\theta}_1 = (\tau_f, Q_{\mathbf{U}}, \lambda, \tau_v, \tau_u, \tau_\delta)$.

Despite the potentially large dimension of the matrix $Q(\boldsymbol{\theta}_1)$, INLA benefits from computation efficiency due to the sparsity of this matrix (Rue et al., 2009).

Moreover, let $\boldsymbol{\theta}_2$ represent the set of hyperparameters directly affecting the observation density, which, in our case, includes only the precision parameter τ_Y . We can restate Equation 6 using the INLA notation as $p(\mathbf{y}_i, \mathbf{x}_i | \mathbf{U}_i, \boldsymbol{\theta}) = \prod_{s=1}^{t_i} p(\mathcal{D}_{i(s)} | \mu_{i(s)}, \boldsymbol{\theta}_2)$. This reformulation allows us to express the overall observation density as $p(\mathcal{D} | \boldsymbol{\mu}, \boldsymbol{\theta}_2) = \prod_i^N \prod_{s=1}^{t_i} p(\mathcal{D}_{i(s)} | \mu_{i(s)}, \boldsymbol{\theta}_2)$, which can be further simplified to $p(\mathcal{D} | \boldsymbol{\mu}, \boldsymbol{\theta}_2) = \prod_{j \in \mathcal{J}} p(\mathcal{D}_j | \mu_j, \boldsymbol{\theta}_2)$ by changing the corresponding indexes. This last expression demonstrates, in line with the requirements of the INLA methodology, that the observation density is conditionally independent.

By denoting the complete set of hyperparameters as $\boldsymbol{\theta} = (\boldsymbol{\theta}_1, \boldsymbol{\theta}_2)$, we recover the same formulation described in Rue et al. (2009). This confirms that the STJM falls within the class of latent Gaussian models, making it suitable for the INLA estimation. More details on how posterior marginals and their corresponding numerical integrations with INLA are computed can be found in Rue et al. (2009); Medina-Olivares et al. (2023b).

2.3 Bayesian model selection with INLA

We aim to select the model that best predicts the full prepayment event of loan i at a given time point t , assuming that the loan has not been repaid up to that time. To compare the predictive performance of different models based on the collected observations, we adopt the methodology proposed by Rizopoulos et al. (2016), which we extend to both the INLA estimation procedure and the STJM formulation.

The authors suggest choosing the model that minimises the cross-entropy of the survival outcome's cross-validated posterior predictive conditional density. Concretely, for each model $M_k \in \{M_1, \dots, M_K\}$ and at time t , we seek to estimate $p(T_i | T_i > t, \mathbf{y}_i(t), \mathcal{D}_{-i}, M_k)$. Here, $\mathbf{y}_i(t)$ represents the historical observations of the longitudinal outcome of loan i up to time t , i.e. $\mathbf{y}_i(t) = \{y_{i,s} : s \leq t\}$, and \mathcal{D}_{-i} denotes the data excluding loan i .

The best model, denoted as $M_{\tilde{k}}$, where $\tilde{k} \in \{1, \dots, K\}$, is determined by minimising the cross-entropy $E(-\log\{p(T_i | T_i > t, \mathbf{y}_i(t), \mathcal{D}_{-i}, M_{\tilde{k}})\})$. The expectation is taken with respect to the model that generated the data, which might not necessarily be one of the K models considered in practice.

To account for the censored cases, Rizopoulos et al. (2016) propose to use the available information and termed this estimate as the *cross-validated Dynamic Conditional Likelihood* (cvDCL) defined as²

$$\text{cvDCL}(t) = \frac{1}{N_t} \sum_{i=1}^N -I(T_i > t) \log\{p(T_i, \delta_i | T_i > t, \mathbf{y}_i(t), \mathcal{D}_{-i})\}, \quad (8)$$

where N_t is the number of loans at risk at time t , i.e. $N_t = \sum_{i=1}^N I(T_i > t)$.

Once the model is estimated, INLA allows generating samples from the approximated posterior density. We propose using this feature to calculate the expression in Equation 8 through Monte Carlo integration, as shown below.

First, note that

$$\frac{p(\boldsymbol{\theta} | T_i, \delta_i, T_i > t, \mathbf{y}_i(t), \mathcal{D}_{-i}) p(T_i, \delta_i | T_i > t, \mathbf{y}_i(t), \mathcal{D}_{-i})}{p(T_i, \delta_i | T_i > t, \mathbf{y}_i(t), \mathcal{D}_{-i}, \boldsymbol{\theta})} = p(\boldsymbol{\theta} | T_i > t, \mathbf{y}_i(t), \mathcal{D}_{-i}),$$

and integration of this last expression with respect to $\boldsymbol{\theta}$ leads to

$$\begin{aligned} p(T_i, \delta_i | T_i > t, \mathbf{y}_i(t), \mathcal{D}_{-i})^{-1} &= \int \frac{p(\boldsymbol{\theta} | T_i, \delta_i, T_i > t, \mathbf{y}_i(t), \mathcal{D}_{-i})}{p(T_i, \delta_i | T_i > t, \mathbf{y}_i(t), \mathcal{D}_{-i}, \boldsymbol{\theta})} d\boldsymbol{\theta} \\ &\approx \int \frac{p(\boldsymbol{\theta} | \mathcal{D})}{p(T_i, \delta_i | T_i > t, \mathbf{y}_i(t), \mathcal{D}_{-i}, \boldsymbol{\theta})} d\boldsymbol{\theta} \\ &\approx \sum_w \frac{\hat{p}(\boldsymbol{\theta}_w | \mathcal{D})}{\hat{p}(T_i, \delta_i | T_i > t, \mathbf{y}_i(t), \mathcal{D}_{-i}, \boldsymbol{\theta}_w)} \Delta_w. \end{aligned} \quad (9)$$

The integration grid $\{\boldsymbol{\theta}_w, \Delta_w\}$ of $\boldsymbol{\theta}$ is constructed by INLA when estimating the model, where Δ_w represents the integration weights.

Moreover, note that the denominator $p(T_i, \delta_i | T_i > t, \mathbf{y}_i(t), \mathcal{D}_{-i}, \boldsymbol{\theta}_w)$ follows

$$\frac{p(\boldsymbol{\mu} | T_i, \delta_i, T_i > t, \mathbf{y}_i(t), \mathcal{D}_{-i}, \boldsymbol{\theta}_w) p(T_i, \delta_i | T_i > t, \mathbf{y}_i(t), \mathcal{D}_{-i}, \boldsymbol{\theta}_w)}{p(T_i, \delta_i | T_i > t, \mathbf{y}_i(t), \boldsymbol{\theta}_w, \boldsymbol{\mu})} = p(\boldsymbol{\mu} | T_i > t, \mathbf{y}_i(t), \mathcal{D}_{-i}, \boldsymbol{\theta}_w),$$

where $\boldsymbol{\mu}$ is the latent field described in Section 2.2. Thus, integrating this last expression with respect to $\boldsymbol{\mu}$ gives

$$\begin{aligned} p(T_i, \delta_i | T_i > t, \mathbf{y}_i(t), \mathcal{D}_{-i}, \boldsymbol{\theta}_w)^{-1} &= \int \frac{p(\boldsymbol{\mu} | T_i, \delta_i, T_i > t, \mathbf{y}_i(t), \mathcal{D}_{-i}, \boldsymbol{\theta}_w)}{p(T_i, \delta_i | T_i > t, \mathbf{y}_i(t), \boldsymbol{\theta}_w, \boldsymbol{\mu})} d\boldsymbol{\mu} \\ &= \int \frac{p(\mathbf{U}_i, \boldsymbol{\mu}_{-\mathbf{U}_i} | T_i, \delta_i, T_i > t, \mathbf{y}_i(t), \mathcal{D}_{-i}, \boldsymbol{\theta}_w)}{p(T_i, \delta_i | T_i > t, \mathbf{y}_i(t), \boldsymbol{\theta}_w, \mathbf{U}_i, \boldsymbol{\mu}_{-\mathbf{U}_i})} d\boldsymbol{\mu}_{-\mathbf{U}_i} d\mathbf{U}_i \\ &\approx \int \frac{p(\mathbf{U}_i | T_i > t, \mathbf{y}_i(t), \boldsymbol{\theta}_w, \boldsymbol{\mu}_{-\mathbf{U}_i}) p(\boldsymbol{\mu}_{-\mathbf{U}_i} | \mathcal{D}, \boldsymbol{\theta}_w)}{p(T_i, \delta_i | T_i > t, \mathbf{y}_i(t), \boldsymbol{\theta}_w, \mathbf{U}_i, \boldsymbol{\mu}_{-\mathbf{U}_i})} d\boldsymbol{\mu}_{-\mathbf{U}_i} d\mathbf{U}_i. \end{aligned}$$

We use the notation $\boldsymbol{\mu} = (\mathbf{U}_i, \boldsymbol{\mu}_{-\mathbf{U}_i})^\top$ to separate the random effects \mathbf{U}_i that strictly depend on the loan i from the rest of the parameters $\boldsymbol{\mu}_{-\mathbf{U}_i}$.

Let $\boldsymbol{\mu}_{-\mathbf{U}_i}^{(r,w)}$ denotes the r th realisation of the approximated posterior sample with $r = 1, \dots, R$, then $p(T_i, \delta_i | T_i > t, \mathbf{y}_i(t), \mathcal{D}_{-i})^{-1}$ from Equation 9, can be estimated as

$$\begin{aligned} p(T_i, \delta_i | T_i > t, \mathbf{y}_i(t), \mathcal{D}_{-i})^{-1} &\approx \sum_w \frac{\hat{p}(\boldsymbol{\theta}_w | \mathcal{D})}{\hat{p}(T_i, \delta_i | T_i > t, \mathbf{y}_i(t), \mathcal{D}_{-i}, \boldsymbol{\theta}_w)} \Delta_w \\ &\approx \sum_w \hat{p}(\boldsymbol{\theta}_w | \mathcal{D}) \Delta_w \int \frac{p(\mathbf{U}_i | T_i > t, \mathbf{y}_i(t), \boldsymbol{\theta}_w, \boldsymbol{\mu}_{-\mathbf{U}_i}) p(\boldsymbol{\mu}_{-\mathbf{U}_i} | \mathcal{D}, \boldsymbol{\theta}_w)}{p(T_i, \delta_i | T_i > t, \mathbf{y}_i(t), \boldsymbol{\theta}_w, \mathbf{U}_i, \boldsymbol{\mu}_{-\mathbf{U}_i})} d\boldsymbol{\mu}_{-\mathbf{U}_i} d\mathbf{U}_i \\ &\approx \sum_w \hat{p}(\boldsymbol{\theta}_w | \mathcal{D}) \Delta_w \left[\frac{1}{R} \sum_r \int \frac{p(\mathbf{U}_i | T_i > t, \mathbf{y}_i(t), \boldsymbol{\theta}_w, \boldsymbol{\mu}_{-\mathbf{U}_i}^{(r,w)})}{p(T_i, \delta_i | T_i > t, \mathbf{y}_i(t), \boldsymbol{\theta}_w, \mathbf{U}_i, \boldsymbol{\mu}_{-\mathbf{U}_i}^{(r,w)})} d\mathbf{U}_i \right]. \end{aligned}$$

²Although we do not explicitly indicate the model k , it is implicitly assumed in the conditioning.

Furthermore, the integral can be calculated, for instance, with empirical Bayes or the Laplace method (Tierney and Kadane, 1986). Whichever method is used to calculate the integral, denote this term as $h_i(\boldsymbol{\theta}_w, \boldsymbol{\mu}_{-\mathbf{U}_i}^{(r,w)}|t)$. Hence, $\widehat{\text{cvDCL}}(t)$ can be estimated as

$$\widehat{\text{cvDCL}}(t)^{INLA} = \frac{1}{N_t} \sum_{i=1}^N I(T_i > t) \times \log \left\{ \sum_w \hat{p}(\boldsymbol{\theta}_w|\mathcal{D}) \Delta_w \left[\frac{1}{R} \sum_r h_i(\boldsymbol{\theta}_w, \boldsymbol{\mu}_{-\mathbf{U}_i}^{(r,w)}|t) \right] \right\}. \quad (10)$$

To get an estimate of the Monte Carlo variance of Equation 10, we use what is known as the *Delta method* (Ver Hoef, 2012). This method approximates a function of random variables using a Taylor series expansion around the means. In our case, we can identify the random variables as $h_{iwr|t} = h_i(\boldsymbol{\theta}_w, \boldsymbol{\mu}_{-\mathbf{U}_i}^{(r,w)}|t)$ which are independent for all the loans i , the integration points w and the realisations r . Denote $m_{iw|t} = \text{E}(h_{iwr|t})$ and $\sigma_{iw|t}^2 = \text{Var}(h_{iwr|t})$ and their estimations, respectively, as $\hat{m}_{iw|t} = \frac{1}{R} \sum_r \hat{h}_{iwr|t}$ and $\hat{\sigma}_{iw|t}^2 = \frac{1}{R-1} \sum_r (\hat{h}_{iwr|t} - \hat{m}_{iw|t})^2$. Then, the first order approximation of $\widehat{\text{cvDCL}}(t)^{INLA}$ as a function of the vector $\mathbf{h}_{|t} = \{h_{iwr|t}\}$ around the vector of means $\mathbf{m}_{|t} = \{m_{iw|t}\}$ is

$$\widehat{\text{cvDCL}}(t)^{INLA} = g(\mathbf{h}_{|t}) \approx g(\mathbf{m}_{|t}) + \sum_{i,w,r} (h_{iwr|t} - m_{iw|t}) \left. \frac{\partial g}{\partial h_{iwr|t}} \right|_{\mathbf{h}_{|t}=\mathbf{m}_{|t}}. \quad (11)$$

Note that by construction $\text{E}(g(\mathbf{h}_{|t})) \approx g(\mathbf{m}_{|t})$. Moreover, the partial derivative terms follow

$$\left. \frac{\partial g}{\partial h_{iwr|t}} \right|_{\mathbf{h}_{|t}=\mathbf{m}_{|t}} = \frac{I(T_i > t)}{N_t} \frac{\hat{p}(\boldsymbol{\theta}_w|\mathcal{D}) \Delta_w}{R \sum_w \hat{p}(\boldsymbol{\theta}_w|\mathcal{D}) \Delta_w \hat{m}_{iw|t}}.$$

Additionally, given that the terms $h_{iwr|t}$ are independent and using the partial derivative expression from above, the variance of the expression in Equation 11 follows

$$\begin{aligned} \text{Var}(\widehat{\text{cvDCL}}(t)^{INLA}) &\approx \sum_{i,w,r} \text{Var}(h_{iwr|t} - m_{iw|t}) \left(\left. \frac{\partial g}{\partial h_{iwr|t}} \right|_{\mathbf{h}_{|t}=\mathbf{m}_{|t}} \right)^2 \\ &= R \sum_{i,w} \hat{\sigma}_{iw|t}^2 \left(\left. \frac{\partial g}{\partial h_{iwr|t}} \right|_{\mathbf{h}_{|t}=\mathbf{m}_{|t}} \right)^2 \\ &= \frac{1}{N_t^2 R} \sum_i I(T_i > t) \frac{\sum_w \hat{\sigma}_{iw|t}^2 (\hat{p}(\boldsymbol{\theta}_w|\mathcal{D}) \Delta_w)^2}{(\sum_w \hat{p}(\boldsymbol{\theta}_w|\mathcal{D}) \Delta_w \hat{m}_{iw|t})^2}. \end{aligned} \quad (12)$$

Thus, Equations 10 and 12 estimate $\widehat{\text{cvDCL}}(t)$ and its variance, respectively.

Initially, Rizopoulos et al. (2016) suggested estimating $\widehat{\text{cvDCL}}(t)$ using posterior samples from an MCMC simulation, which is explained in detail in Appendix A. To assess the appropriateness of our estimate compared to the authors', we conducted a comparative analysis using simulated datasets described in Appendix B.

3 Empirical analysis on US mortgage prepayment

3.1 Data

We use the publicly available Single Family Loan-Level Dataset provided by Freddie Mac³. This dataset contains comprehensive mortgage information, including loan-level details, application covariates, and monthly performance data.

The dataset consists of loans granted from June, 2015 to November, 2015, with monthly performance records tracked until December 2019. The mortgage with the longest time record is 4.5 years (54 months). The dataset considers 57,258 borrowers with a total of 2,559,056 observations. During the study period, 16,239 borrowers opted to prepay their mortgage loans fully. Figure 1 shows the distribution of full prepayment events over time.

The time-fixed covariates represented by the vector \mathbf{z}_i in Equation 2 are as follows

³Data can be accessed at <https://www.freddiemac.com/research/datasets/sf-loanlevel-dataset>

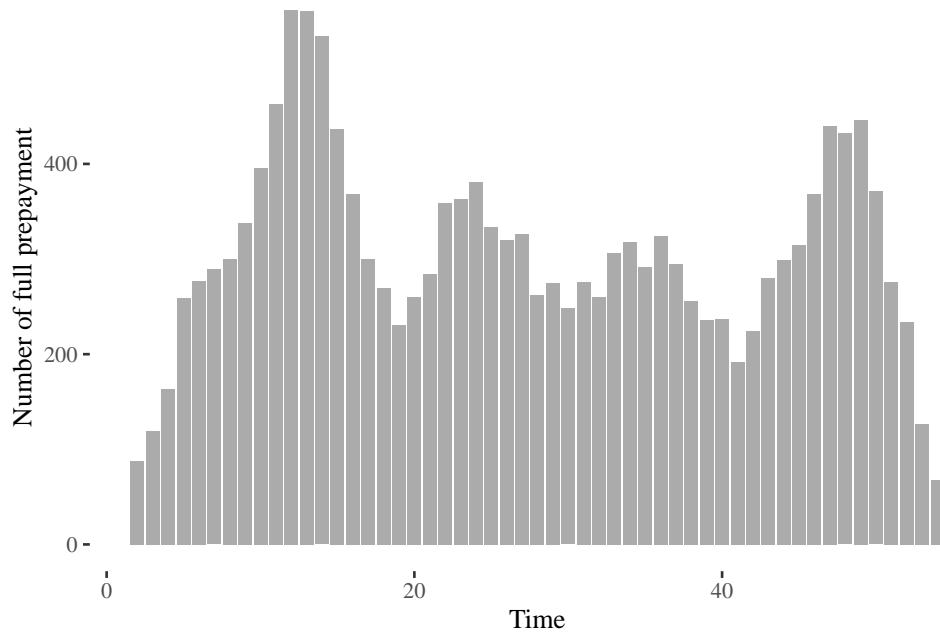


Figure 1: Distribution of full prepayment events over time.

- **cltv** is the loan-to-value ratio based on the original mortgage loan amount plus any other mortgage loan amount divided by the property’s purchase price.
- **orig_upb** is the original unpaid principal balance of the mortgage on the note date.
- **cnt_units** denotes whether the mortgage is a one- (= 1, 93% of the loans) or more than one-unit property (= 0, 7% of the loans).
- **dti** is the debt-to-income ratio. It corresponds to the borrower’s monthly debt payments divided by the total monthly income used to underwrite the loan.
- **int_rt** is the interest rate given at the origination of the credit.
- **term** corresponds to the number of scheduled monthly mortgage payments. It is divided between short-term loans, with terms less than or equal to 15 years (= 0, 19% of the loans) and long-term loans, with terms greater than 15 years (= 15, 81% the loans).
- **loan_purpose** indicates whether the mortgage loan purpose is a cash-out refinance loan (= 0, 22% of the loans)⁴, no cash-out refinance loan (= N, 25% of the loans) or purchase (= P, 53% of the loans).
- **cnt_borr** is the number of borrowers obligated to repay the mortgage. Either one borrower (= 0, 48% of the loans) or more than one (= 2, 52% of the loans).

These covariates are commonly used in similar contexts, as seen in studies such as Wang et al. (2020) and Hu and Zhou (2019), which also employ this dataset.

Table 1 shows descriptive statistics of the numeric covariates defined above. As a pre-processing step, these variables are standardised to have a zero-mean and standard deviation of 1.

Concerning the longitudinal outcome, we are interested in a simple variable that indicates early repayments. Medina-Olivares et al. (2023b) show a correlation between borrowers who pay more than the due amount and the prepayment event for a dataset on consumer loans. For this empirical analysis, we follow the same rationale of looking for a candidate variable that measures the distance between what has been paid and what has been due. For simplicity, we look for a variable that shows a simple functional structure, such as a linear relationship, to facilitate the longitudinal design and, therefore, the model estimation.

⁴A cash-out refinance mortgage loan is a loan in which the use of the amount is not limited to specific purposes.

Covariate	N	Mean	SD	$Q_{2.5\%}$	$Q_{25\%}$	$Q_{50\%}$	$Q_{75\%}$	$Q_{95\%}$
cltv(%)	57258	73.50	16.97	38.00	65.00	79.00	85.00	95.00
orig_upb*	57258	256.32	121.87	88.00	161.00	241.00	336.00	475.00
dti(%)	57258	34.87	9.14	19.00	28.00	36.00	42.00	48.00
int_rt(%)	57258	3.93	0.44	3.00	3.75	4.00	4.25	4.62

*1,000 USD.

Table 1: Descriptive statistics for numeric covariates in the dataset.

Assume that for a generic loan, we denote the interest rate given at origination as i with a monthly instalment equal to A . Then, the sum of the total amount paid until time t , including the capitalisation of the inflows, is $A + A(1+i) + \dots + A(1+i)^{t-1}$. Since the interest rate for mortgage loans is low for the analysed time period⁵, we can apply a first-order Maclaurin approximation (around zero) with respect to i , so we obtain $At + At(t-1)i/2$. For the first periods, the linear term of this expression dominates.

To make the longitudinal outcome comparable across different loans, we define it as $y_t = \sum_{s=0}^{t-1} (1+i)^s / T$. T represents the study period, which is 54 months in our analysis. The sole purpose of including T in the expression is for scaling. Note that by geometric series equivalence, the following expression also holds $y_t = \frac{(1+i)^t - 1}{iT}$. If the total amount paid by the borrower is greater than the due amount at time t , then the observed y_t should have a larger slope against time than the theoretical curve.

In the dataset, we can access the observed unpaid principal balance at any given time. Since this amount may deviate from the scheduled balance, we aim to express y_t in terms of this variable. Let's denote the unpaid principal balance at the loan's origination as P_0 , the current unpaid principal balance at time t as P_t , and the loan term as M . Therefore, using fundamental instalment relationships, we can derive an equivalent expression for y_t as

$$y_t = \frac{(P_0 - P_t)(1+i)^M - 1}{P_0 iT}.$$

Therefore, y_t represents a longitudinal outcome with a simple structural form that can be expressed in terms of the observed flows.

Figure 2 shows our dataset's longitudinal outcome. To facilitate visualisation, mortgage loans that experienced prepayment are in a red dashed line, and those that do not are in a blue dotted line.

Regarding geographical information, properties are located in 8 states: New York, New Jersey, Connecticut, Massachusetts, Rhode Island, Maine, New Hampshire and Vermont. These states are divided into 123 areas given by the first three digits of the zip code. The number of loans distributed among these areas is shown in the map of Figure 3.

In addition, Figure 4 shows the corresponding full prepayment rates, calculated as the total number of events divided by the number of granted loans in each area. From this figure, although the rates include all events regardless of when they occurred, spatial clustering is observed and can be considered a first check to support the inclusion of spatial effects.

3.2 Models and results

Following the methodology described in Section 2.2, we estimate three joint models with different specifications. All these three specifications include the same time-fixed covariates described in Section 3.1 and the same structure of the longitudinal outcome (see below). The differences come rather from the baseline specifications $\nu_{a,s}$ (see Equation 2). Concretely, the longitudinal outcome follows

$$\begin{aligned} Y_{i,s} | \eta_{Y_{i,s}}, \tau_Y &\sim N(\eta_{Y_{i,s}}, \tau_Y^{-1}) \\ \eta_{Y_{i,s}} &= \beta_{01} + \beta_{11}s + U_{0i} + U_{1i}s \\ (U_{0i}, U_{1i})^\top &\sim N_2(0, Q_U^{-1}), \end{aligned} \tag{13}$$

⁵The 95% quantile of the annual interest rate is 4.62%, which represents a monthly interest rate of 0.0038%. See Table 1.

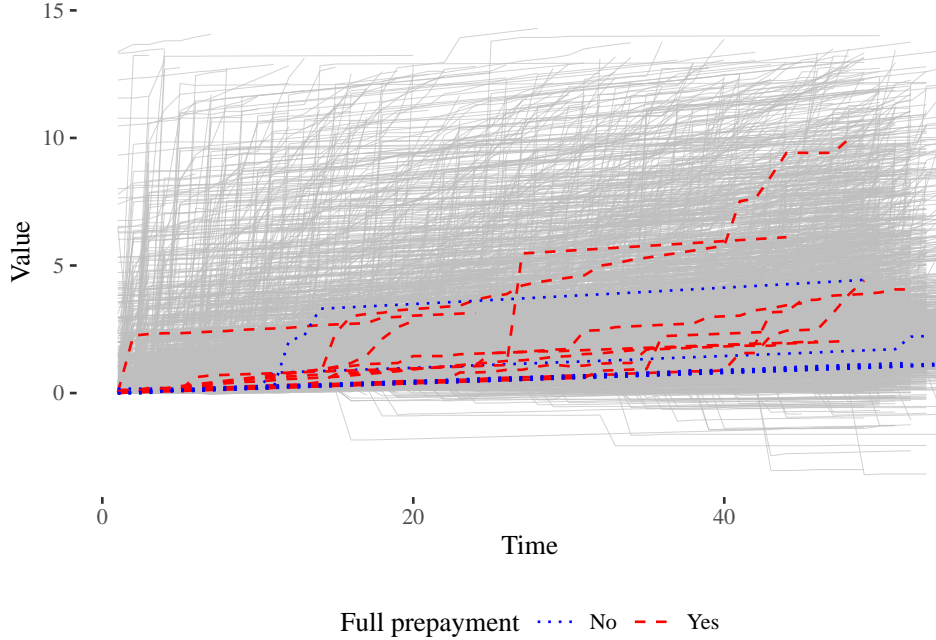


Figure 2: Evolution of the longitudinal outcomes. Borrowers that experience prepayment are in dashed red line, and borrowers that are censored in blue dotted line.

where the covariance matrix Q_U^{-1} is parameterised via marginal precisions τ_{U_0} and τ_{U_1} , and the pairwise correlation ρ_{01} as follows

$$Q_U^{-1} = \begin{pmatrix} 1/\tau_{U_0} & \rho_{01}/\sqrt{\tau_{U_0}\tau_{U_1}} \\ \rho_{01}/\sqrt{\tau_{U_0}\tau_{U_1}} & 1/\tau_{U_1} \end{pmatrix}. \quad (14)$$

The mixed-effect model from Equation 13 is known as intercept-slope random effects. This specification is justified because the longitudinal outcome approximates a linear trend when the interest rate is low, as shown in Section 3.1. Moreover, the survival process for the three models follow

$$\begin{aligned} X_{i,s} | \eta_{X_{i,s}} &\sim \text{Bernoulli}(\text{logit}^{-1}(\eta_{X_{i,s}})) \\ \eta_{X_{i,s}} &= \nu_{a_{i,s}} + \mathbf{z}_i^\top \boldsymbol{\beta}_2 + \lambda(U_{0i} + U_{1i}s), \end{aligned} \quad (15)$$

where $\nu_{a_{i,s}}$ is the baseline risk.

Table 2 describes the three models' specifications for $\nu_{a,s}$. M_1 is a discrete-time joint model, similar to the ones analysed in Medina-Olivares et al. (2023a) (univariate, without autoregressive terms). M_2 introduces a novel aspect to the literature as there are no existing studies on joint models with spatial main effects in discrete time. The closest model to M_2 is a joint model that includes the spatial main effects in a Weibull survival component suggested by Martins et al. (2016). Finally, M_3 is the model that encompasses all the effects (the temporal and spatial main effects as well as the interactions).

Id	Temporal Effects	Spatial Effects	S-T Interactions	$\nu_{a,s}$
M_1	Yes	No	No	$\nu_0 + v_s$
M_2	Yes	Yes	No	$\nu_0 + v_s + u_a$
M_3	Yes	Yes	Yes	$\nu_0 + v_s + u_a + \delta_{a,s}$

Table 2: Specification of the joint models. M_1 includes the temporal effects in the baseline hazard. M_2 considers both the temporal and the spatial main effects, and M_3 captures both the temporal and the spatial main effects in addition to their interactions.

Table 3 shows the parameter estimates for the three models. We observe that the parameters strictly associated with the longitudinal outcome, β_{01} and β_{11} , are consistent among M_1 , M_2 and M_3 . However, we

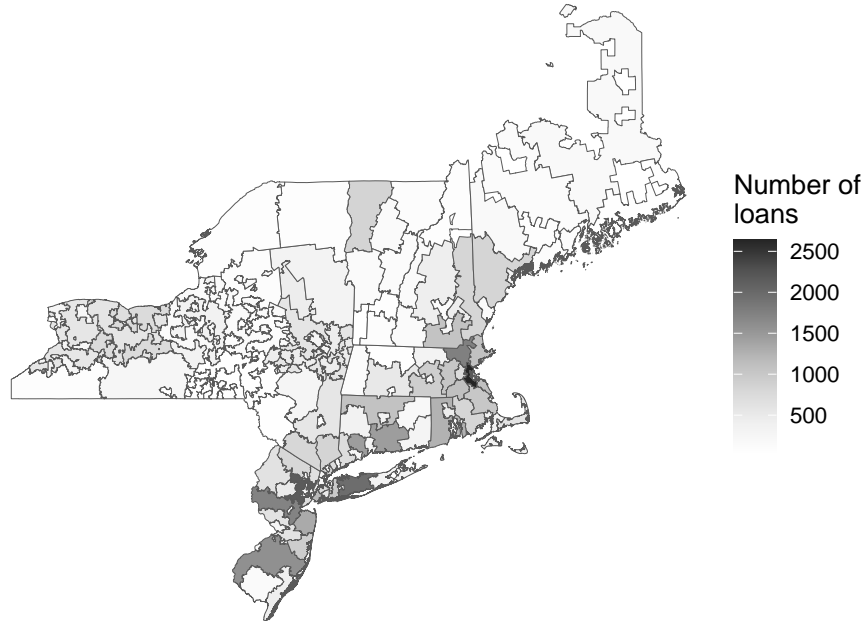


Figure 3: Number of loans distributed by area.

notice differences in the covariates associated with the survival process. For instance, the coefficient related to $cltv$ under the estimation of M_1 is 0.301, and its 95% posterior credible interval does not include zero. The positive sign suggests that the higher the $cltv$, the greater the probability of prepaying in full. Yet, when estimated under specifications M_2 and M_3 , although the sign remains positive, the effect of this covariate decreases and is not as significant as before.

In the same line, we notice that the effect of $diti$ for M_1 shows a negative relationship with the prepayment. Similar results were found in Medina-Olivares et al. (2023b) for the consumer loans dataset. However, when we include the spatial effects, either with M_2 or M_3 , the relation of high $diti$ with a low probability of full prepayment is not entirely conclusive, even shifting the posterior marginals to the positive values.

For the other covariates, we found consistent results among the three models. For example, the original unpaid principal balance, $orig_upb$, shows a positive relationship with the prepayment, which is also supported by the prepayment models from Medina-Olivares et al. (2023b). Moreover, it is less likely to prepay in full if the mortgage is more than a one-unit property (cnt_units), if the loan term is longer than 15 years ($term_g15$), if the number of borrowers is greater than 1 (cnt_borr2) or if the purpose of the loan is to purchase rather than refinance ($loan_purpose$).

The interest rate granted at origination, int_rt , is expected to play an essential role in the decision of full prepayment. If the reference interest rates fall compared to the one granted, it is more attractive to renegotiate the credit. As seen in Table 3 for all three models, its positive effect suggests that the higher the interest rate given at origination, the greater the probability of full prepayment. This has also been seen in Medina-Olivares et al. (2023b). However, when we include the spatial effects, we note that the associated coefficient also increases.

Regarding λ , the parameter that associates the random effects of the longitudinal outcome and the survival process, we observe that the three models estimate a significant positive association, as expected, since the more is paid off from what is owed, the more likely it is to prepay in full. However, the magnitude of the estimate differs among the models. The largest one is due to M_1 with a mean of 0.201. When we add the spatial main effects in M_2 , we see a mean decrease to 0.146. Yet, when we add the spatio-temporal interactions in M_3 , we observe a value in between, with a mean of 0.171.

Furthermore, we obtained similar results among the three models regarding the hyperparameters associated with the longitudinal outcome. Namely, the precision of the error terms τ_Y and the elements τ_{U_0} , τ_{U_1} and ρ_{01} of the precision matrix Q_U . However, the precision of the temporal main effects τ_v changes among the three

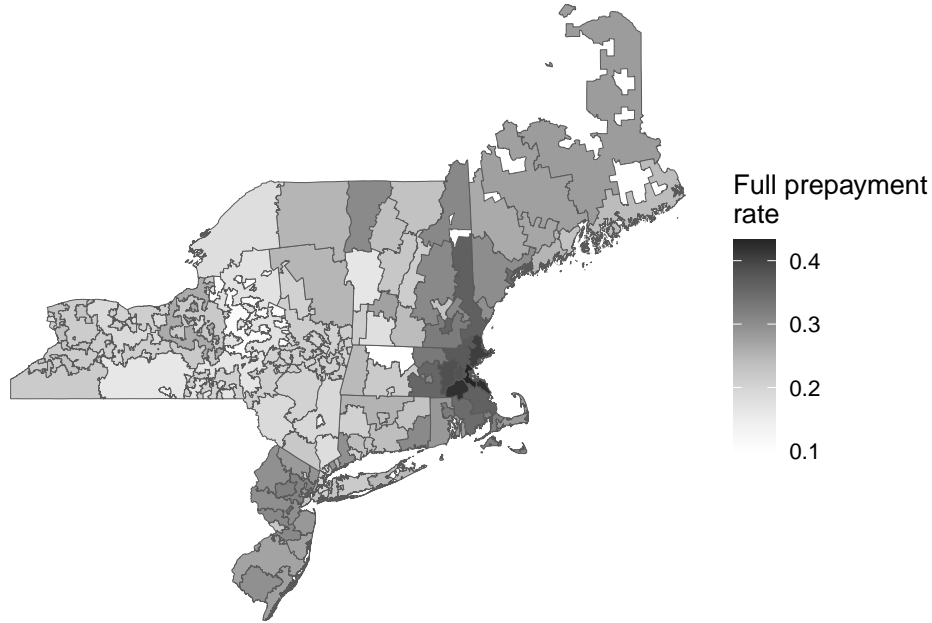


Figure 4: Full prepayment rate distributed by area.

	M_1			M_2			M_3		
	Mean	2.5%	97.25%	Mean	2.5%	97.25%	Mean	2.5%	97.25%
β_{01}	0.011	0.008	0.013	0.011	0.008	0.013	0.011	0.008	0.013
β_{11}	0.027	0.026	0.027	0.027	0.026	0.027	0.027	0.026	0.027
ν_0	-8.247	-8.451	-8.043	-8.590	-8.798	-8.382	-8.541	-8.748	-8.334
cltv	0.301	0.081	0.520	0.114	-0.120	0.347	0.117	-0.115	0.349
orig_upb	0.143	0.128	0.159	0.153	0.134	0.172	0.153	0.134	0.172
cnt_units1	0.439	0.367	0.510	0.425	0.351	0.499	0.408	0.334	0.482
dti	-0.109	-0.222	0.005	0.024	-0.091	0.139	0.018	-0.097	0.132
int_rt	0.794	0.743	0.845	0.869	0.817	0.921	0.846	0.794	0.898
term_g15	-0.458	-0.518	-0.399	-0.531	-0.591	-0.470	-0.518	-0.579	-0.458
loan_purposeN	0.028	-0.018	0.074	-0.005	-0.051	0.041	-0.010	-0.056	0.036
loan_purposeP	-0.137	-0.180	-0.093	-0.100	-0.144	-0.057	-0.109	-0.153	-0.066
cnt_borr2	-0.060	-0.091	-0.028	-0.061	-0.093	-0.029	-0.063	-0.095	-0.031
λ	0.201	0.188	0.211	0.146	0.139	0.156	0.171	0.162	0.184
τ_Y	34.713	34.653	34.777	34.715	34.656	34.783	34.784	34.730	34.826
τ_{U_0}	9.651	9.568	9.752	9.627	9.557	9.716	9.870	9.767	9.956
τ_{U_1}	895.736	885.777	904.230	887.034	874.223	898.767	880.029	871.477	890.400
ρ_{01}	-0.067	-0.076	-0.058	-0.052	-0.060	-0.046	-0.056	-0.064	-0.051
τ_v	3.004	2.245	3.653	2.435	1.369	3.375	0.802	0.518	1.094
τ_u				16.667	12.163	25.503	14.777	12.806	17.464
τ_δ							104.613	57.088	196.704

Table 3: Parameter estimates for models M_1 , M_2 and M_3 .

models. We see a mean of 3.004, 2.435 and 0.802 for models M_1 , M_2 and M_3 , respectively. That raises the question of how different each model's estimated temporal main effects are. Figure 5 shows the estimated temporal main effects for the three models. Models M_1 and M_2 overlap for much of the study period, and M_3 shows some differences, in particular for the first periods, but overall, the effect of the three models is fairly comparable.

To compare the performance of the models, we follow the procedure described in Section 2.3. We estimate the $\widehat{cvDCL}(t)^{INLA}$ (Equation 10) for six evaluation times t , ranging from 12 to 42 months with an increment of

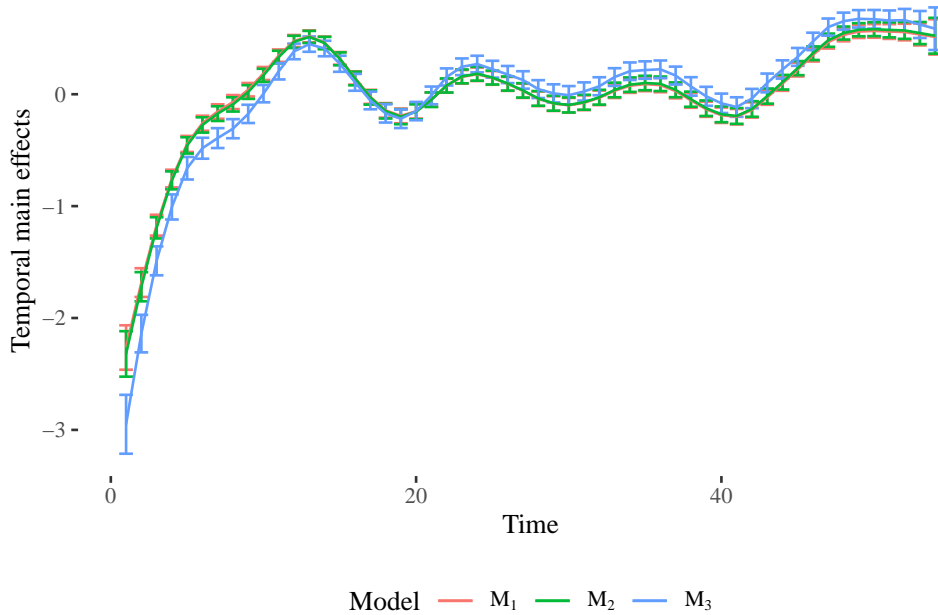


Figure 5: Temporal main effects estimated by the three models. The error bars represent the estimated 95% credible intervals.

6 months. The results are shown in Table 4 (we deliberately omit the word “INLA” to shorten the notation). N_t is the number of borrowers at risk, and the values in brackets are the estimates of Monte Carlo standard error derived from Equation 12. It is worth noting that the metric value should be compared across the models for one value of t , that is, all the values that belong to the same row since, between the rows, there is an evident overlap of datasets. The table shows that both M_2 and M_3 outperform M_1 . Adding the latent spatial component can increase the model’s performance for this dataset. However, when we compare models M_2 and M_3 , that is, when we add on top of the spatial main effects, the spatio-temporal interactions, the improvements are not as clear as before.

	N_t	M_1	M_2	M_3
$\widehat{cvDCL}(t = 12)$	53963	1.4438 (5.69e-06)	1.4244 (1.03e-05)	1.4304 (5.72e-05)
$\widehat{cvDCL}(t = 18)$	51489	1.2231 (4.01e-06)	1.2143 (7.57e-06)	1.2165 (2.20e-05)
$\widehat{cvDCL}(t = 24)$	49607	1.0349 (3.58e-06)	1.0306 (6.91e-06)	1.0310 (1.35e-05)
$\widehat{cvDCL}(t = 30)$	47839	0.8472 (3.27e-06)	0.8450 (6.40e-06)	0.8448 (1.15e-05)
$\widehat{cvDCL}(t = 36)$	46059	0.6453 (2.91e-06)	0.6438 (5.68e-06)	0.6439 (1.08e-05)
$\widehat{cvDCL}(t = 42)$	44611	0.4656 (2.52e-06)	0.4644 (4.96e-06)	0.4648 (1.00e-05)

Table 4: Comparison of model performance. The value in brackets is an estimate of the Monte Carlo standard error.

To further explore the analysis, we assign the overall $\widehat{cvDCL}(t)$ to the corresponding area and compare from which areas the major gains are obtained for models M_2 and M_3 with respect to model M_1 . Figure 6 shows two maps for the segmented \widehat{cvDCL} evaluated at $t = 12$. The left corresponds to the difference between M_2 and M_1 ($M_2 - M_1$), and the right one to $M_3 - M_1$. From both maps, we observe that the major contributions to the overall metric mainly come from the middle-left (west, Rochester area) and middle-right parts (east, Boston area) of the maps. These differences are increased for model M_2 .

Moreover, when we choose a different evaluation time, for instance, $t = 24$ (see Figure 7), now the contributions coming from the Rochester area are not as meaningful as for $t = 12$. Instead, the differences come from New Jersey, New York City and Boston locations. Thus, when we include spatial effects, we see that the consistent

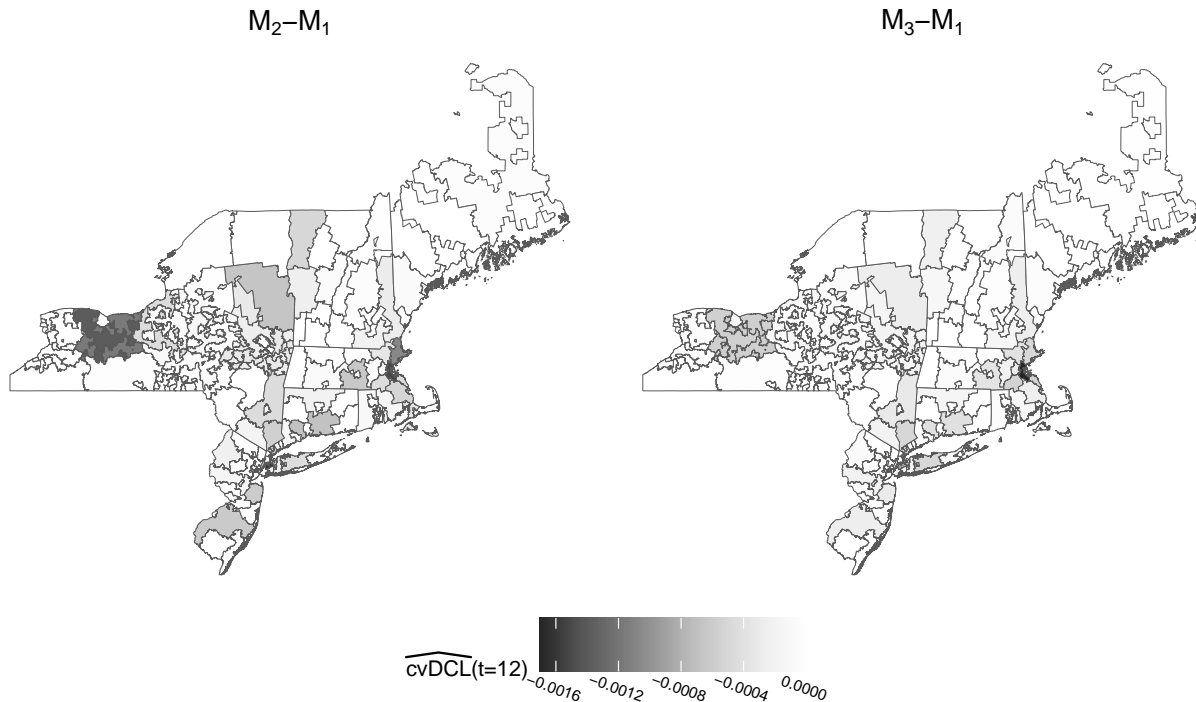


Figure 6: Difference between the $\widehat{cvDCL}(t = 12)$ for models M_2 and M_3 with respect to M_1 and segmented by area.

improvements in the performance evaluated in different periods are not exclusively attributed to a particular area.

4 Discussion

Previous studies have shown that the joint model approach offers advantages over the widely used survival approaches in credit-related applications (Hu and Zhou, 2019; Medina-Olivares et al., 2023a,b). In this manuscript, we extend this existing research by investigating enhanced representations of the survival predictor. Specifically, we incorporate spatial and spatio-temporal effects into the baseline hazard and explore how this modification can impact the prediction performance of a prepayment model for US mortgages. This decision is supported by two main factors. Firstly, there is evidence from previous research that incorporating spatial effects into credit risk models can result in improved predictions (Calabrese and Crook, 2020; Medina-Olivares et al., 2022). Secondly, as mentioned earlier, the joint modelling of longitudinal and survival processes offers an attractive dynamic prediction framework for credit modelling.

In this respect, we make four main contributions. First, we introduce the Spatio-Temporal Joint Model (STJM), a Bayesian joint model formulated in discrete time that includes a flexible baseline hazard in the survival predictor. The baseline hazard is effectively decomposed into temporal and spatial main effects, along with their interactions. For this latter, we leverage the approach from Clayton (1996) in which the structure matrix is built by the Kronecker product of the main effects structure matrices. Moreover, we follow the Goicoa et al. (2018) approach to get appropriate identifiability constraints by using spectral decomposition over the structure matrices.

Second, to estimate the STJM in a large dataset, we formulate the model using the INLA methodology (Rue et al., 2009) and implement it in the R-INLA package (<https://www.r-inla.org/>). This implementation allows us to scale the model to a dataset with 57,258 borrowers with 2,559,056 total observations. As far as we know, this is the largest sample size used in a joint model application.

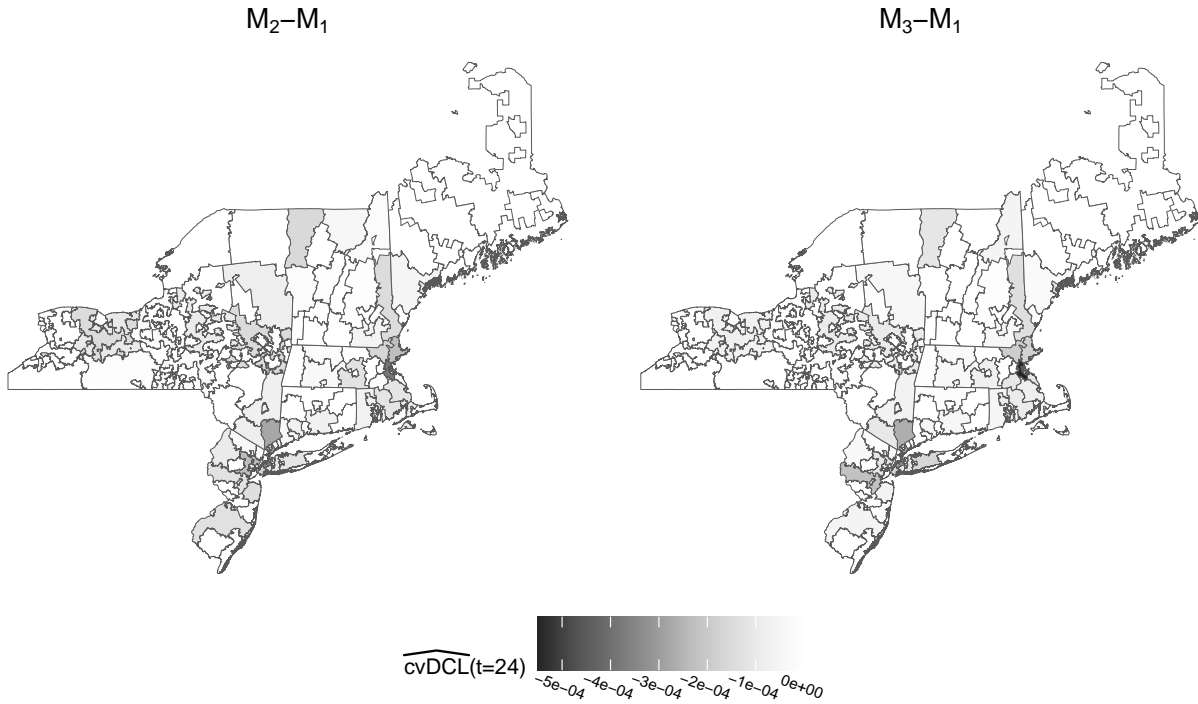


Figure 7: Difference between the $\widehat{\text{cvDCL}}(t = 24)$ for models M_2 and M_3 with respect to M_1 and segmented by area.

Third, we propose a modified version of the *cross-validated Dynamic Conditional Likelihood* originally proposed by Rizopoulos et al. (2016). Our adaptation leverages the estimations obtained through the INLA methodology, which differs from the original version that relies on posterior MCMC samples, resulting in reduced computational costs. We compare the original and the proposed versions by a simulation study that demonstrates adequate results (see Appendix B).

Fourth, we apply the proposed approach to predict the full prepayment event in US mortgage loans. The analysis comprises three models: (1) measuring only the temporal main effect (M_1), (2) adding the temporal and spatial main effects (M_2), and (3) incorporating both main effects along with their interactions (M_3). In general, the parameter estimates show agreement across the three joint models. However, a notable difference arises concerning the covariate “debt to income ratio” (*dti*), which represents the sum of the borrower’s monthly debt payments divided by their monthly income. When spatial effects are excluded, the parameter estimate indicates that higher *dti* values are associated with a lower probability of prepayment. However, this relationship no longer holds when spatial effects are included.

Additionally, the empirical results reveal that spatial effects consistently enhance the prediction performance of the joint model across all evaluation times. Interestingly, when we contrast the performance evaluated at different time intervals, these improvements are not limited to a specific region. However, including spatio-temporal interactions does not yield equally clear performance gains compared to the model without such interactions.

Our robust findings, facilitated by the suitability of INLA estimation for large datasets, suggest that mortgage grantors could improve predictive performance in practice by employing the proposed spatial approach. Potential impacts may involve the refinement of methodologies for estimating cash flows for credit loss provisioning purposes and the identification of optimal levels of economic capital, ultimately leading to a more competitive and prudent risk assessment.

This study presents compelling insights that undoubtedly pave the way for further research. One avenue worth exploring is the inclusion of TVCs whose processes do not need to be jointly estimated with a dependent variable. These TVCs could encompass macroeconomic variables, allowing us to investigate how changes in the overall economic conditions impact the joint model’s performance. Comparable approaches have been adopted in credit survival models (Bellotti and Crook, 2009; Djeundje and Crook, 2018; Dirick et al., 2019), corporate credit default models (Li et al., 2022) and a time-continuous joint model without spatial effects (Hu and Zhou, 2019). Since these TVCs are external factors, we can assume that the occurrence of a specific event does not influence their trajectories. Consequently, there is no need for a borrower-specific longitudinal model for these covariates. This could lead to a more comprehensive joint model framework, leveraging individual predictions while incorporating the influence of economic conditions.

References

- Allison, P. D. (1982). Discrete-time methods for the analysis of event histories. *Sociological Methodology*, 13:61–98.
- Banerjee, S., Carlin, B. P., and Gelfand, A. E. (2014). *Hierarchical modeling and analysis for spatial data*. CRC Press.
- Bellotti, T. and Crook, J. (2009). Credit scoring with macroeconomic variables using survival analysis. *Journal of the Operational Research Society*, 60(12):1699–1707.
- Besag, J., York, J., and Mollié, A. (1991). Bayesian image restoration, with two applications in spatial statistics. *Annals of the Institute of Statistical Mathematics*, 43(1):1–20.
- Calabrese, R. (2023). Contagion effects of UK small business failures: A spatial hierarchical autoregressive model for binary data. *European Journal of Operational Research*, 305(2):989–997.
- Calabrese, R. and Crook, J. (2020). Spatial contagion in mortgage defaults: a spatial dynamic survival model with time and space varying coefficients. *European Journal of Operational Research*, 287(2):749–761.
- Carlin, B. P. and Louis, T. A. (2000). *Bayes and empirical Bayes methods for data analysis*. Chapman & Hall/CRC, Boca Raton.
- Chang, H. H., Reich, B. J., and Miranda, M. L. (2013). A spatial time-to-event approach for estimating associations between air pollution and preterm birth. *Journal of the Royal Statistical Society: Series C (Applied Statistics)*, 62(2):167–179.
- Clayton, D. G. (1996). Generalized linear mixed models. *Markov chain Monte Carlo in practice*, 1:275–302.
- Crook, J. and Bellotti, T. (2010). Time varying and dynamic models for default risk in consumer loans. *Journal of the Royal Statistical Society: Series A (Statistics in Society)*, 173(2):283–305.
- Dirick, L., Bellotti, T., Claeskens, G., and Baesens, B. (2019). Macro-economic factors in credit risk calculations: including time-varying covariates in mixture cure models. *Journal of Business & Economic Statistics*, 37(1):40–53.
- Djeundje, V. B. and Crook, J. (2018). Incorporating heterogeneity and macroeconomic variables into multi-state delinquency models for credit cards. *European Journal of Operational Research*, 271(2):697–709.
- Fahrmeir, L. and Tutz, G. (1994). *Multivariate Statistical Modelling Based on Generalized Linear Models*, volume 425. Springer, New York, NY.
- Freni-Sterrantino, A., Ventrucci, M., and Rue, H. (2018). A note on intrinsic conditional autoregressive models for disconnected graphs. *Spatial and Spatio-temporal Epidemiology*, 26:25–34.
- Gelfand, A. E., Ghosh, S. K., Knight, J. R., and Sirmans, C. F. (1998). Spatio-temporal modeling of residential sales data. *Journal of Business & Economic Statistics*, 16(3):312–321.
- Gelman, A., Carlin, J. B., Stern, H. S., Dunson, D. B., Vehtari, A., and Rubin, D. B. (2013). *Bayesian Data Analysis*. CRC Press.
- Goicoa, T., Adin, A., Ugarte, M., and Hodges, J. (2018). In spatio-temporal disease mapping models, identifiability constraints affect PQL and INLA results. *Stochastic Environmental Research and Risk Assessment*, 32(3):749–770.
- Goodstein, R., Hanouna, P., Ramirez, C. D., and Stahel, C. W. (2017). Contagion effects in strategic mortgage defaults. *Journal of Financial Intermediation*, 30:50–60.
- Guiso, L., Sapienza, P., and Zingales, L. (2013). The determinants of attitudes toward strategic default on mortgages. *The Journal of Finance*, 68(4):1473–1515.

- Gupta, A. (2019). Foreclosure contagion and the neighborhood spillover effects of mortgage defaults. *The Journal of Finance*, 74(5):2249–2301.
- Henderson, R., Diggle, P., and Dobson, A. (2000). Joint modelling of longitudinal measurements and event time data. *Biostatistics*, 1(4):465–480.
- Hu, W. and Zhou, J. (2019). Joint modeling: an application in behavioural scoring. *Journal of the Operational Research Society*, 70(7):1129–1139.
- Iversen Jr, E. S. (2001). Spatially disaggregated real estate indices. *Journal of Business & Economic Statistics*, 19(3):341–357.
- Knorr-Held, L. (2000). Bayesian modelling of inseparable space-time variation in disease risk. *Statistics in Medicine*, 19(17-18):2555–2567.
- Laird, N. M. and Ware, J. H. (1982). Random-effects models for longitudinal data. *Biometrics*, 38(4):963–974.
- Li, S., Tian, S., Yu, Y., Zhu, X., and Lian, H. (2022). Corporate probability of default: A single-index hazard model approach. *Journal of Business & Economic Statistics*, pages 1–12.
- Lindgren, F. and Rue, H. (2008). On the second-order random walk model for irregular locations. *Scandinavian Journal of Statistics*, 35(4):691–700.
- Martins, R., Silva, G. L., and Andreozzi, V. (2016). Bayesian joint modeling of longitudinal and spatial survival AIDS data. *Statistics in Medicine*, 35(19):3368–3384.
- Medina-Olivares, V., Calabrese, R., Crook, J., and Lindgren, F. (2023a). Joint models for longitudinal and discrete survival data in credit scoring. *European Journal of Operational Research*, 307(3):1457–1473.
- Medina-Olivares, V., Calabrese, R., Dong, Y., and Shi, B. (2022). Spatial dependence in microfinance credit default. *International Journal of Forecasting*, 38(3):1071–1085.
- Medina-Olivares, V., Lindgren, F., Calabrese, R., and Crook, J. (2023b). Joint models of multivariate longitudinal outcomes and discrete survival data with INLA: An application to credit repayment behaviour. *European Journal of Operational Research*, 310(2):860–873.
- Pence, K. M. (2006). Foreclosing on opportunity: State laws and mortgage credit. *Review of Economics and Statistics*, 88(1):177–182.
- Ratcliffe, S. J., Guo, W., and Ten Have, T. R. (2004). Joint modeling of longitudinal and survival data via a common frailty. *Biometrics*, 60(4):892–899.
- Rizopoulos, D. (2012). *Joint models for longitudinal and time-to-event data: With applications in R*. CRC Press.
- Rizopoulos, D., Taylor, J. M., Van Rosmalen, J., Steyerberg, E. W., and Takkenberg, J. J. (2016). Personalized screening intervals for biomarkers using joint models for longitudinal and survival data. *Biostatistics*, 17(1):149–164.
- Rue, H. and Held, L. (2005). *Gaussian Markov random fields: theory and applications*. CRC Press.
- Rue, H., Martino, S., and Chopin, N. (2009). Approximate Bayesian inference for latent gaussian models by using integrated nested Laplace approximations. *Journal of the Royal Statistical Society: Series B (Statistical Methodology)*, 71(2):319–392.
- Schrödle, B. and Held, L. (2011). Spatio-temporal disease mapping using INLA. *Environmetrics*, 22(6):725–734.
- Thomas, L., Crook, J., and Edelman, D. (2017). *Credit scoring and its applications*. Society for Industrial and Applied Mathematics.
- Tierney, L. and Kadane, J. B. (1986). Accurate approximations for posterior moments and marginal densities. *Journal of the American Statistical Association*, 81(393):82–86.
- Towe, C. and Lawley, C. (2013). The contagion effect of neighboring foreclosures. *American Economic Journal: Economic Policy*, 5(2):313–35.
- Tsiatis, A. A. and Davidian, M. (2004). Joint modeling of longitudinal and time-to-event data: an overview. *Statistica Sinica*, 14(3):809–834.
- Ver Hoef, J. M. (2012). Who invented the delta method? *The American Statistician*, 66(2):124–127.
- Wang, Z., Crook, J., and Andreeva, G. (2020). Reducing estimation risk using a Bayesian posterior distribution approach: Application to stress testing mortgage loan default. *European Journal of Operational Research*, 287(2):725–738.

Wulfsohn, M. S. and Tsiatis, A. A. (1997). A joint model for survival and longitudinal data measured with error. *Biometrics*, pages 330–339.

Zhou, H., Lawson, A. B., Hebert, J. R., Slate, E. H., and Hill, E. G. (2008). Joint spatial survival modeling for the age at diagnosis and the vital outcome of prostate cancer. *Statistics in Medicine*, 27(18):3612–3628.

A Estimation of cvDCL under MCMC scheme

In Section 2.3, we show how the *cross-validated Dynamic Conditional Likelihood* (cvDCL) is estimated using the INLA methodology. Here, we describe how the cvDCL is computed with an MCMC sampling scheme. This is done for comprehensive understanding since in Appendix B, we compare numerically how different these two approaches are using simulation analysis.

From Equation 8, we know

$$\text{cvDCL}(t) = \frac{1}{N_t} \sum_{i=1}^N -I(T_i > t) \log\{p(T_i, \delta_i | T_i > t, \mathbf{y}_i(t), \mathcal{D}_{-i})\},$$

where $N_t = \sum_{i=1}^N I(T_i > t)$ (the number of loans at risk at time t). It can be shown that (see Rizopoulos et al., 2016, for further details)⁶

$$p(T_i, \delta_i | T_i > t, \mathbf{y}_i(t), \mathcal{D}_{-i})^{-1} \approx \int \frac{p(\mathbf{U}_i, \Theta | \mathcal{D})}{p(T_i, \delta_i | T_i > t, \mathbf{y}_i(t), \mathbf{U}_i, \Theta)} d\Theta d\mathbf{U}_i, \quad (16)$$

where Θ is the set of all parameters as described in Section 2.2 and \mathbf{U}_i the random effects for loan i . Let $\Theta^{(g)}$ and $\mathbf{U}_i^{(g)}$ denote the g -th realisation of the posterior sample with $g = 1, \dots, G$, then $p(T_i, \delta_i | T_i > t, \mathbf{y}_i(t), \mathcal{D}_{-i})^{-1}$ can be estimated by

$$\hat{p}(T_i, \delta_i | T_i > t, \mathbf{y}_i(t), \mathcal{D}_{-i})^{-1} = \frac{1}{G} \sum_{g=1}^G \frac{1}{p(T_i, \delta_i | T_i > t, \mathbf{y}_i(t), \mathbf{U}_i^{(g)}, \Theta^{(g)})}.$$

Hence, cvDCL(t) can be computed as

$$\widehat{\text{cvDCL}}(t)^{MCMC} = \frac{1}{N_t} \sum_{i=1}^N I(T_i > t) \log \left\{ \frac{1}{G} \sum_{g=1}^G \frac{1}{p(T_i, \delta_i | T_i > t, \mathbf{y}_i(t), \mathbf{U}_i^{(g)}, \Theta^{(g)})} \right\}. \quad (17)$$

We estimate the variance of $\widehat{\text{cvDCL}}(t)^{MCMC}$ through batching (Carlin and Louis, 2000). This requires that a long run of G samples is divided into M successive batches of size H (i.e. $G = M \cdot H$). For each batch $m = 1, \dots, M$, we calculate $\widehat{\text{cvDCL}}(t)_m^{MCMC}$ using its H posterior samples, and the variance is then the sample variance of these M estimations.

B Comparison cvDCL: MCMC and INLA

Here, we study how different is the estimation of the cvDCL between the MCMC and INLA procedures (Equations 17 from Appendix A and 10 from Section 2.3, respectively). To this end, we first generate data from a joint model that follows Equations 18 and 19 for the longitudinal and event processes, respectively.

$$\begin{aligned} Y_{i,s} | \eta_{Y_{i,s}}, \tau_Y &\sim N(\eta_{Y_{i,s}}, \tau_Y^{-1}) \\ \eta_{Y_{i,s}} &= \beta_{01} + U_{0i} + (\beta_{11} + U_{1i})s, \\ (U_{0i}, U_{1i})^\top &\sim N_2(\mathbf{0}, \mathbf{Q}_U^{-1}), \end{aligned} \quad (18)$$

$$\begin{aligned} X_{i,s} | \eta_{X_{i,s}} &\sim \text{Bernoulli}(\text{logit}^{-1}(\eta_{X_{i,s}})) \\ \eta_{X_{i,s}} &= \nu_0 + v_s + \beta_{12}z_{1i} + \beta_{22}z_{2i} + \lambda(U_{0i} + U_{1i}s), \\ v_s &\sim RW2(\tau_v). \end{aligned} \quad (19)$$

⁶In that work, Equation 16 is presented as equality. We confirmed with the author that there is an error and that it should be an approximation symbol instead.

Next, we estimate the $\widehat{\text{cvDCL}}(t)^{MCMC}$ and $\widehat{\text{cvDCL}}(t)^{INLA}$, for different values of t , assuming two different specifications of the joint model. The first specification is the correct one, i.e. follows Equations 18 and 19. The second one omits the second covariate in the event predictor. Specifically, it assumes the linear predictor of the event process as $\nu_0 + v_s + \beta_{11}z_{1i} + \lambda(U_{0i} + U_{1i}s)$ (see Equation 19). By comparing the cvDCL values under these two distinct settings, we not only gain insights into their differences but also assess how the cvDCL varies when one specification outperforms the other in explaining the data.

Table 5 shows the results of the comparative analysis. The INLA implementation is presented in two ways, one calculates $h_i(\boldsymbol{\theta}_w, \boldsymbol{\mu}_{-U_i}^{(r,w)} | t)$ (see Section 2.3) with the Laplace method (INLA Lap) and the other with empirical Bayes (INLA EB).

	Correct Specification			
	N_t	MCMC	INLA Lap	INLA EB
$\widehat{\text{cvDCL}}(t = 12)$	424	2.5915 (6.80e-04)	2.5922	2.5778
$\widehat{\text{cvDCL}}(t = 18)$	347	2.4715 (6.75e-04)	2.4716	2.4679
$\widehat{\text{cvDCL}}(t = 24)$	183	2.3951 (8.66e-04)	2.3942	2.3930
$\widehat{\text{cvDCL}}(t = 30)$	85	2.1884 (1.63e-03)	2.1857	2.1864
$\widehat{\text{cvDCL}}(t = 36)$	36	1.7153 (4.22e-03)	1.7085	1.7115
	Other Specification			
	N_t	MCMC	INLA Lap	INLA EB
$\widehat{\text{cvDCL}}(t = 12)$	424	2.8023 (7.34e-04)	2.8027	2.7949
$\widehat{\text{cvDCL}}(t = 18)$	347	2.6893 (7.95e-04)	2.6890	2.6874
$\widehat{\text{cvDCL}}(t = 24)$	183	2.6037 (1.27e-03)	2.6027	2.6031
$\widehat{\text{cvDCL}}(t = 30)$	85	2.3634 (1.70e-03)	2.3598	2.3632
$\widehat{\text{cvDCL}}(t = 36)$	36	1.8390 (4.27e-03)	1.8305	1.8382

Table 5: Comparison of model performance for simulated data and two different specifications.